Supplemental material

Supplemental Figures and Tables

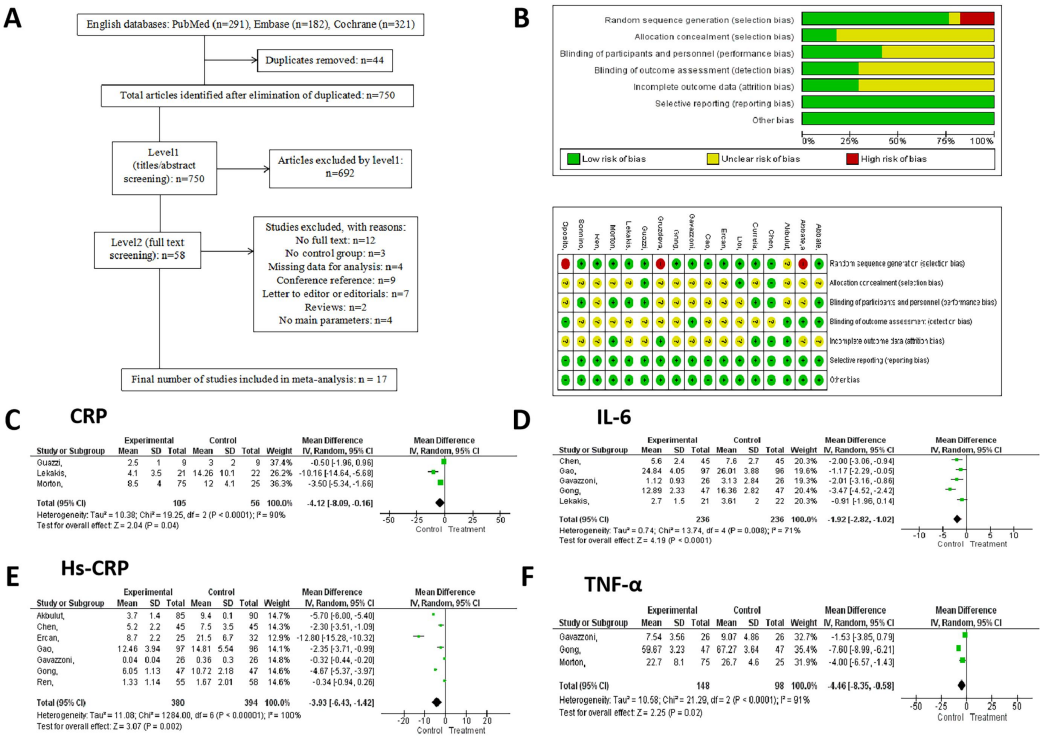

Figure S1. Meta-analysis of clinical studies of acute myocardial infarction (AMI)-related inflammation treatment over the past 20 years. (**A**): Flowchart of literature search and study selection process. (**B**): Evaluation of quality of retrieved studies. (**C-F**): Meta-analysis of levels of inflammatory factors (C-reactive protein, interleukin-6, high-sensitivity C-reactive protein, and tumor necrosis factor alpha) in serum of AMI patients.

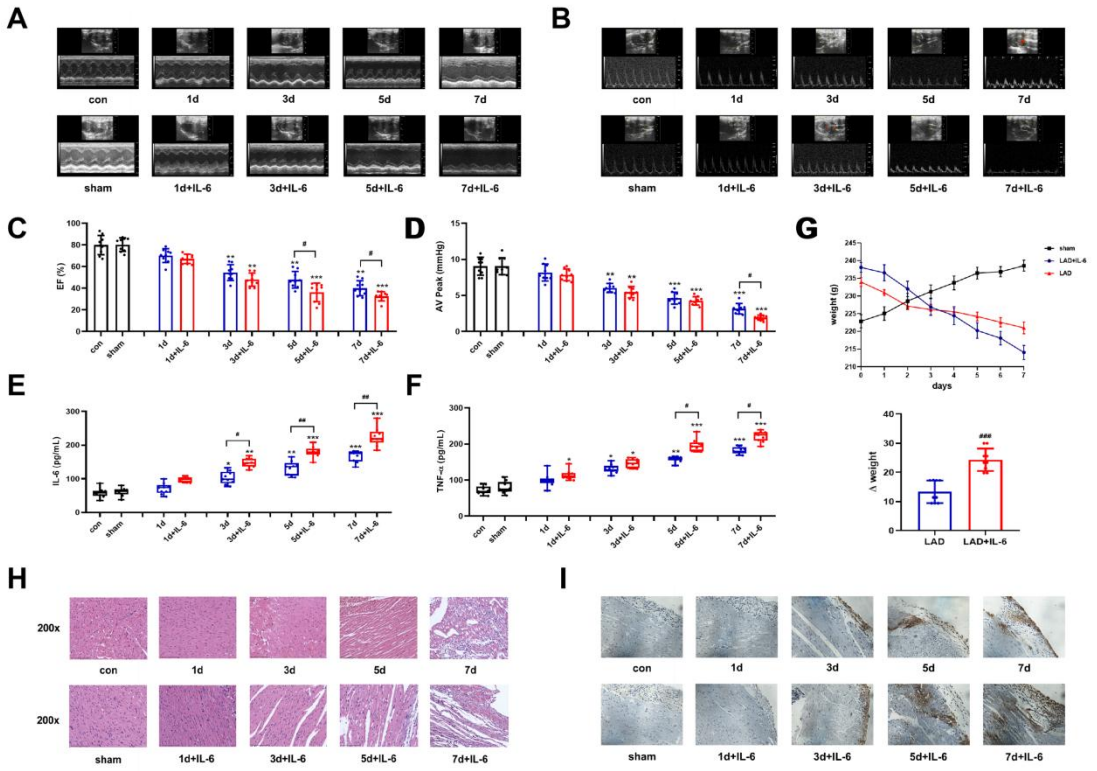

Figure S2. Inflammation aggravates progression of acute myocardial infarction. (**A**-**B**): Effect of interleukin-6 (IL-6) on cardiac functionality in rats with the left anterior descending (LAD) coronary artery ligation. (**C**-**D**): Quantitative assessment of dilation and systolic function based on left ventricular ejection fraction and arteriovenous peak. (**E**-**F**): Levels of serum inflammatory cytokines (IL-6 and tumor necrosis factor alpha) in rat LAD model. The levels of inflammatory cytokines were determined using enzyme-linked immunosorbent assays. (**G**): Effect of IL-6 on change in weight of LAD rats. (**H**): Representative photomicrographs of hematoxylin and eosin-stained myocardia from LAD rats with or without IL-6 (200×). (**I**): Evaluation of the effect of IL-6 on cardiomyocyte injury in LAD rats using terminal deoxynucleotidyl transferase dUTP nick-end labeling staining (200×). Data are expressed as means ± SEM, n = 9 in each group; $^{*}P < 0.05$, $^{**}P < 0.01$, $^{***}P < 0.001$ versus sham; $^{\#}P < 0.05$, $^{\#\#}P < 0.01$, $^{\#\#\#}P < 0.001$ versus LAD groups. Unpaired Student's t-test for comparing two groups, and two-way ANOVA was used for comparing multiple groups.

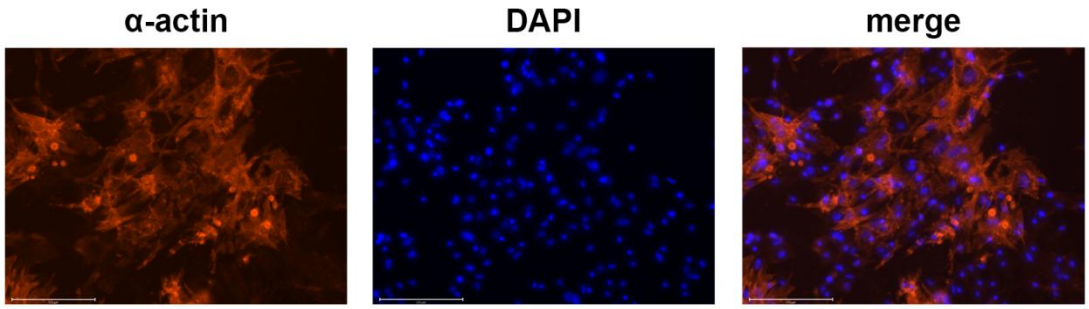

Figure S3. α-actin staining of rat primary cardiac cells.

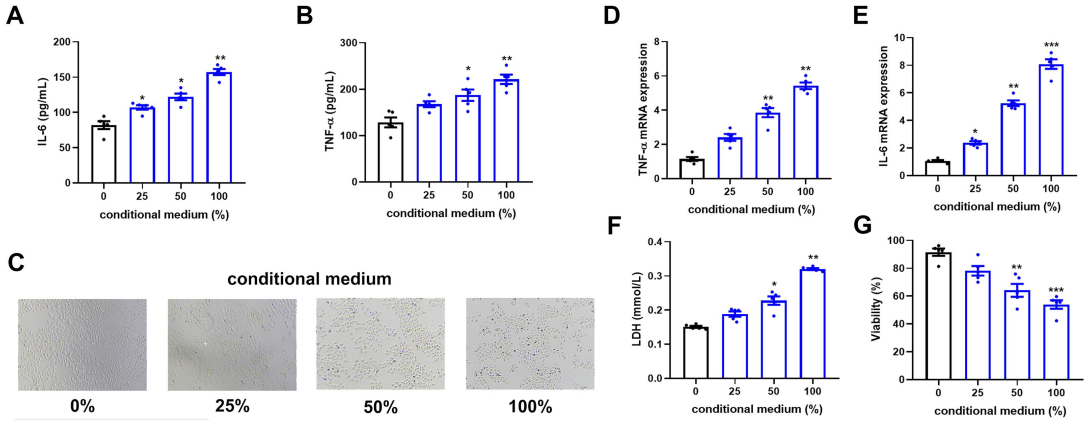

Figure S4. Inflammatory factors aggravate cardiomyocyte damage. (A-B): Expression of inflammatory factors in conditioned media at different concentrations. (**C**): Influence of conditioned medium on cell state. (**D-E**): Expression of inflammatory factors in co-cultured cells. (**F-G**): Changes in cell viability in co-cultured cells. Data are expressed as means ± SEM, n = 5 in each group; $^{*}P < 0.05$, $^{**}P < 0.01$, $^{***}P < 0.001$ versus control. Unpaired Student's t-test for comparing two groups.

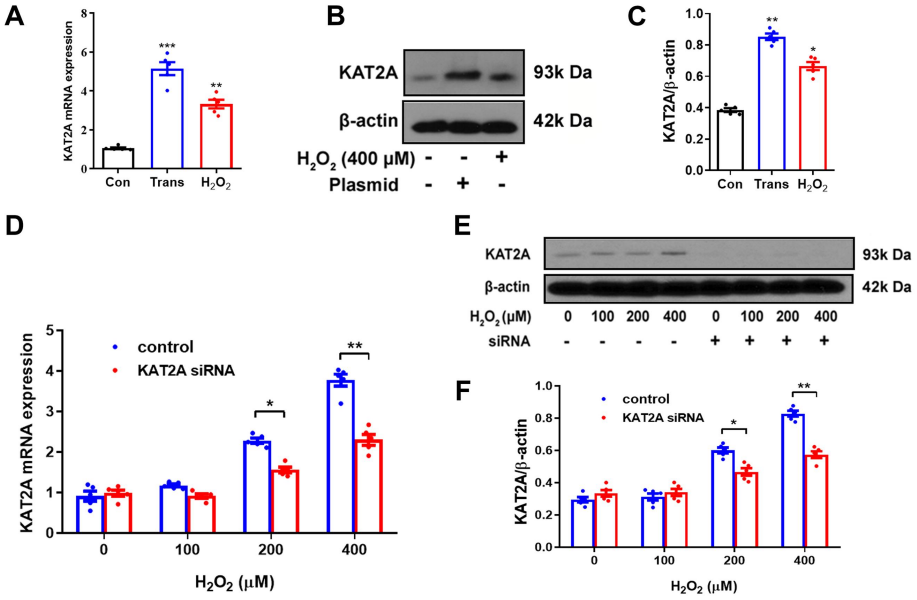

Figure S5. KAT2A expression in cardiomyocyte after transfection. (**A-C**): KAT2A expression increased in cells after transfection with KAT2A plasmid. (**D-F**): KAT2A expression decreased in cells after transfection with KAT2A siRNA. Data are expressed as means ± SEM, n = 5 in each group; $^{*}P < 0.05$, $^{**}P < 0.01$ versus non-siRNA group. Unpaired Student's t-test for comparing two groups, and two-way ANOVA was used for comparing multiple groups.

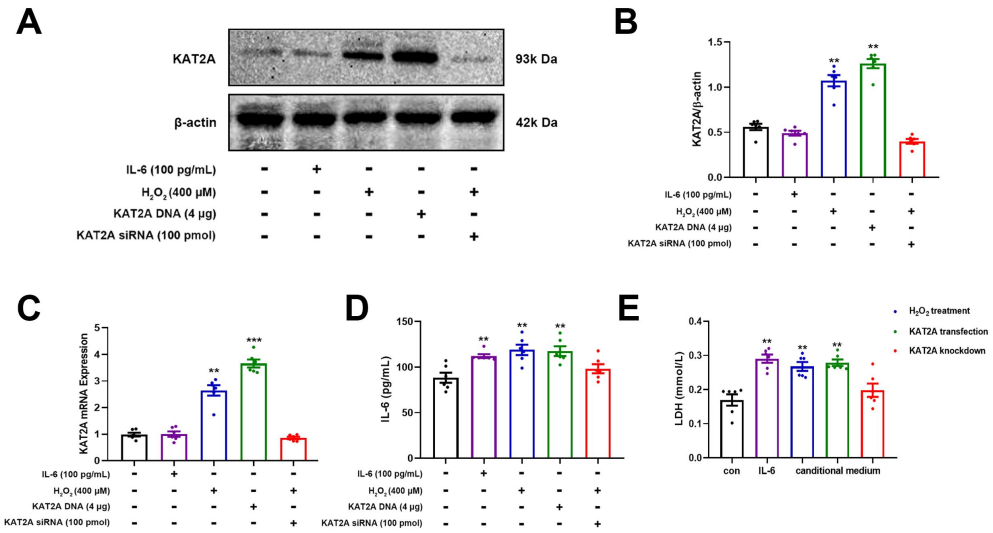

Figure S6. KAT2A involves in the cardiomyocytic injury. (**A-C**): KAT2A protein and mRNA expression in cells following treatment under various conditions. (**D**): Interleukin-6 expression in cell culture medium after treatment under various conditions. (**E**): Lactate dehydrogenase expression in co-cultured cells. Data are expressed as means ± SEM, n = 6 in each group; $^{**}P < 0.01$, $^{***}P < 0.001$ versus control. Unpaired Student's t-test for comparing two groups, and two-way ANOVA was used for comparing multiple groups.

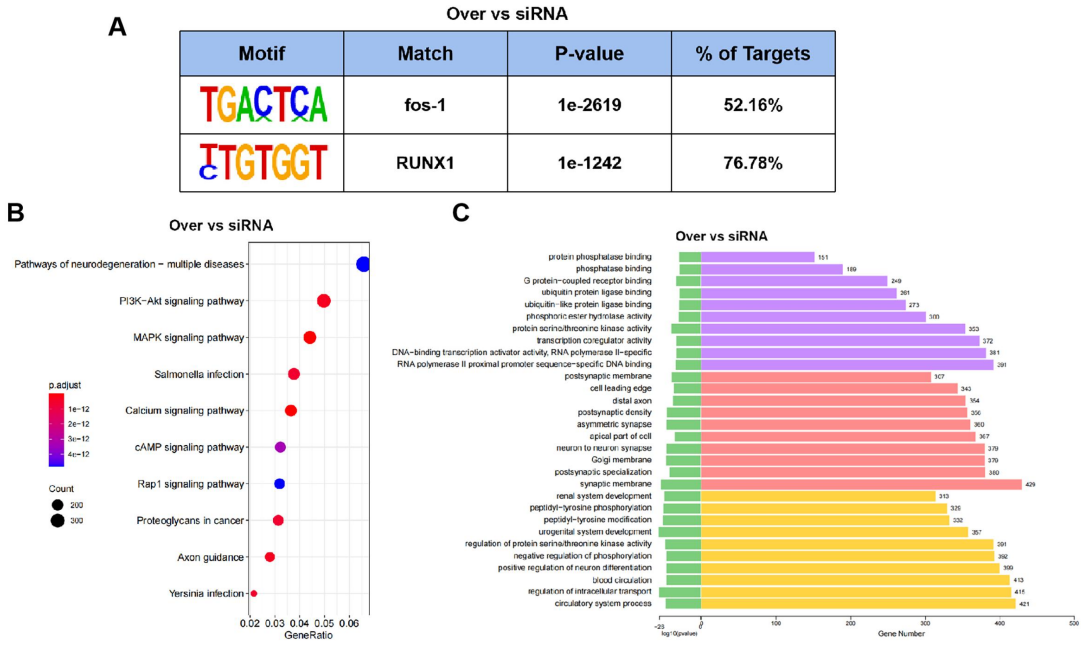

Figure S7. ATAC-seq differential peak analysis (overexpression vs. siRNA group). (**A**): Motif enrichment analysis. (**B**): Kyoto Encyclopedia of Genes and Genomes enrichment analysis. (**C**): Gene ontology enrichment analysis.

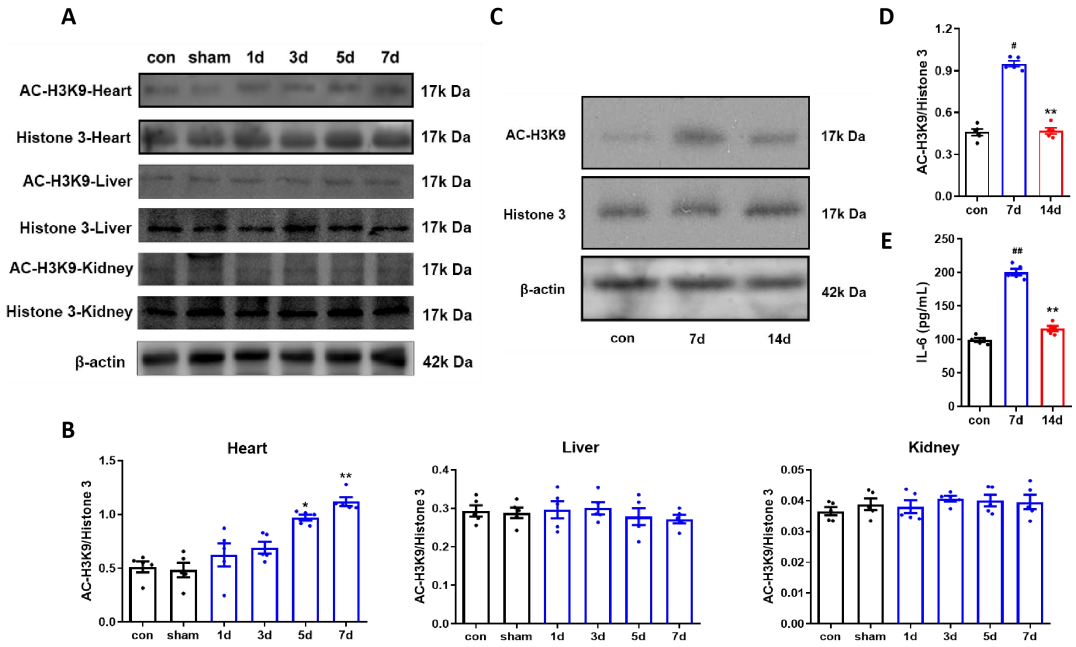

Figure S8. KAT2A activity increases in the heart after acute myocardial infarction. (**A-B**): Changes in expression of AC-H3K9 (in heart, liver and kidney) in left anterior descending (LAD) model. (**C-D**): Change in expression of heart AC-H3K9 in LAD model after 14 days. (**E**): Level of interleukin-6 in LAD model rat serum after 14 days. Data are expressed as means ± SEM, n = 5 in each group; $^{*}P < 0.05$, $^{**}P < 0.01$, $^{***}P < 0.001$ versus sham. Unpaired Student's t-test for comparing two groups, and two-way ANOVA was used for comparing multiple groups.

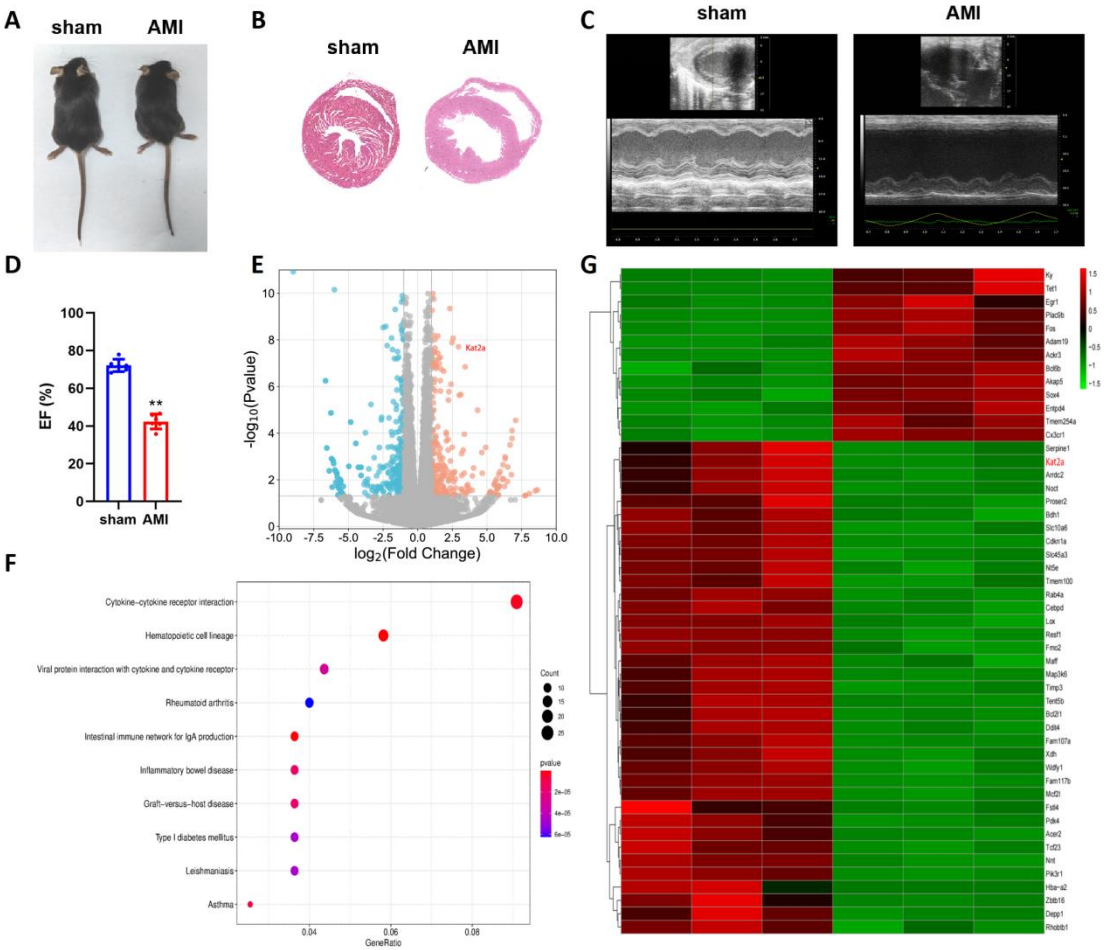

Figure S9. The expression of KAT2A in myocardium of AMI mice was significantly increased. (**A**): Changes of mice physical signs before and after AMI. (**B**): Representative photomicrographs of hematoxylin and eosin-stained myocardia from LAD mice (scan). (**C-D**): Cardiac functionality in mice with LAD coronary artery ligation. (**E**): RNA-seq of expression of differential genes in mice before and after LAD coronary artery ligation. (**F**): Distribution of differential genes in GSEA. (**G**): Most significantly regulated genes (Top 50) grouped by clustering analysis.

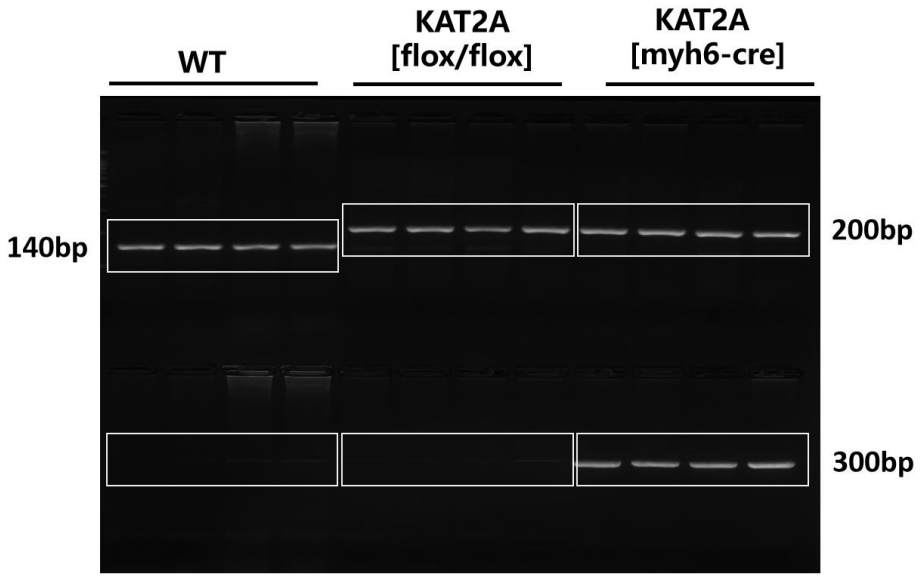

Figure S10. Results of KAT2A$^{-/-}$ mice genotyping. The augmented genetic fragments of only 140 bp is from wild-type (WT) mice; the augmented genetic fragment of only 200 bp is from KAT2A [flox/flox] mice; and the augmented genetic fragments of 200 and 300 bp are from KAT2A$^{-/-}$ mice.

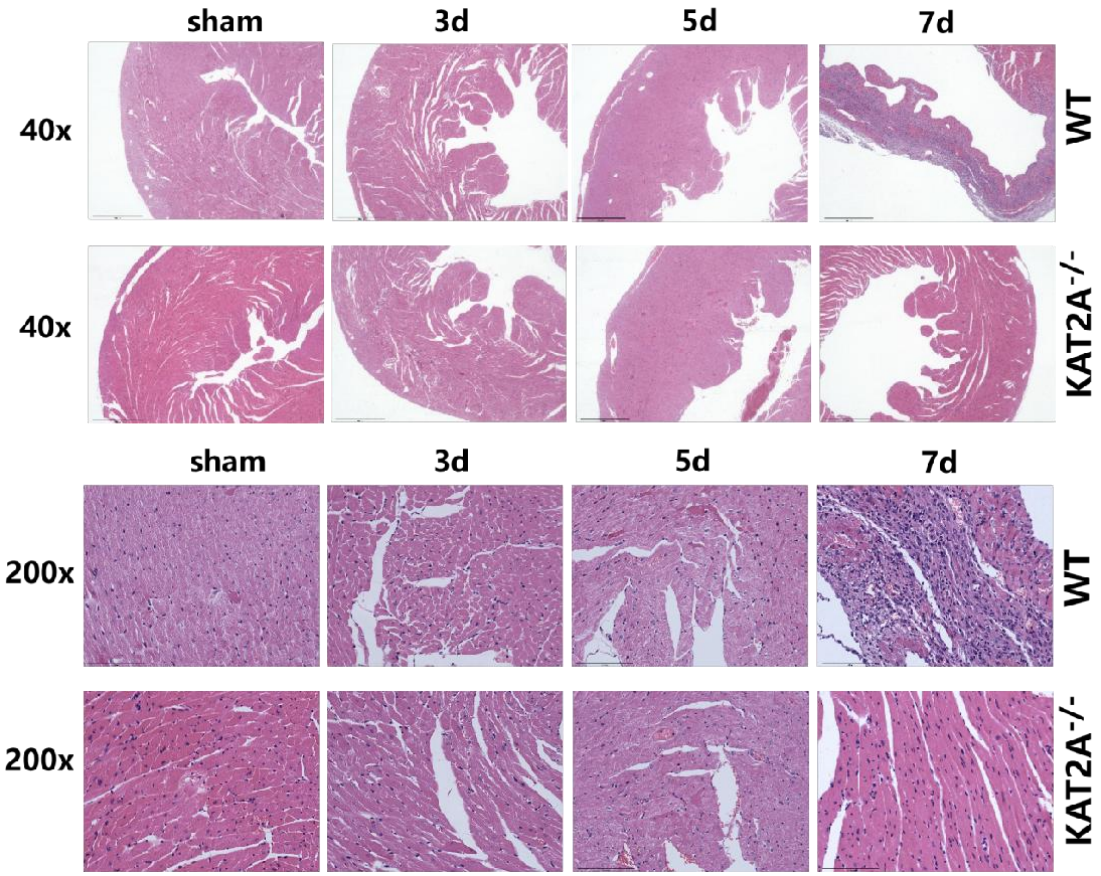

Figure S11. Pathological staining of myocardia from left anterior descending (LAD) mice in wild-type (WT) and KAT2A$^{-/-}$ groups. Representative photomicrographs of hematoxylin and eosin-stained myocardia from LAD mice in WT and KAT2A$^{-/-}$ groups (40× and 200×, respectively).

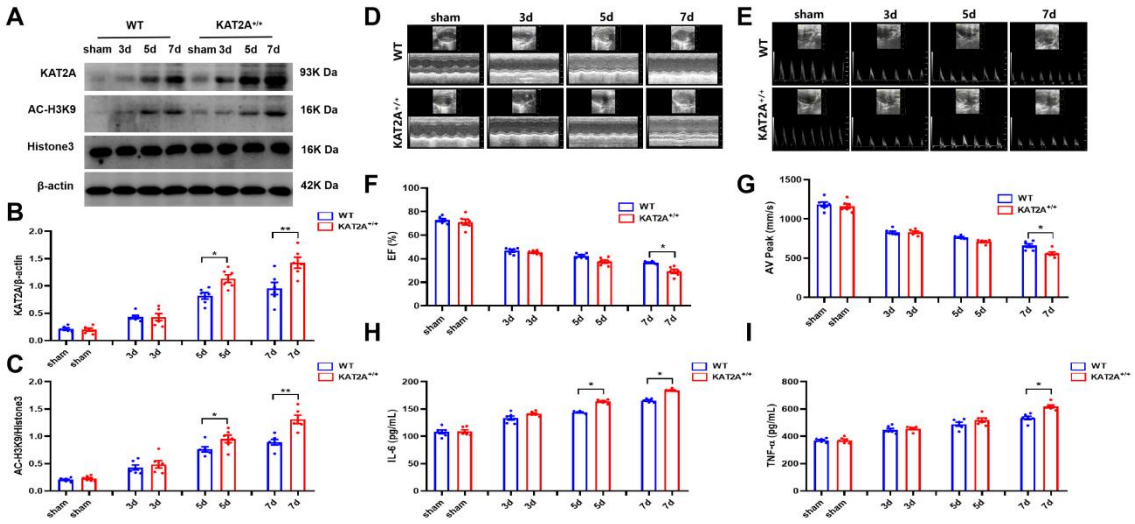

Figure S12. KAT2A promotes the development of AMI. (**A-C**): Changes in expression of KAT2A and AC-H3K9 in WT and KAT2A$^{+/+}$ mice. (**D-E**): Cardiac functionality in KAT2A$^{+/+}$ mice with left anterior descending (LAD) coronary artery ligation. (**F-G**): Quantitative assessment of dilation and systolic function based on left ventricular ejection fraction and arteriovenous peak. (**H-I**): Changes in levels of serum inflammatory cytokines (interleukin-6 and tumor necrosis factor alpha) in LAD model mice. The levels of inflammatory cytokines were determined using enzyme-linked immunosorbent assays. Data are expressed as means ± SEM, n = 6 in each group; $^{*}P < 0.05$,$^{**}P < 0.01$, versus WT groups. Unpaired Student's t-test for comparing two groups, and two-way ANOVA was used for comparing multiple groups.

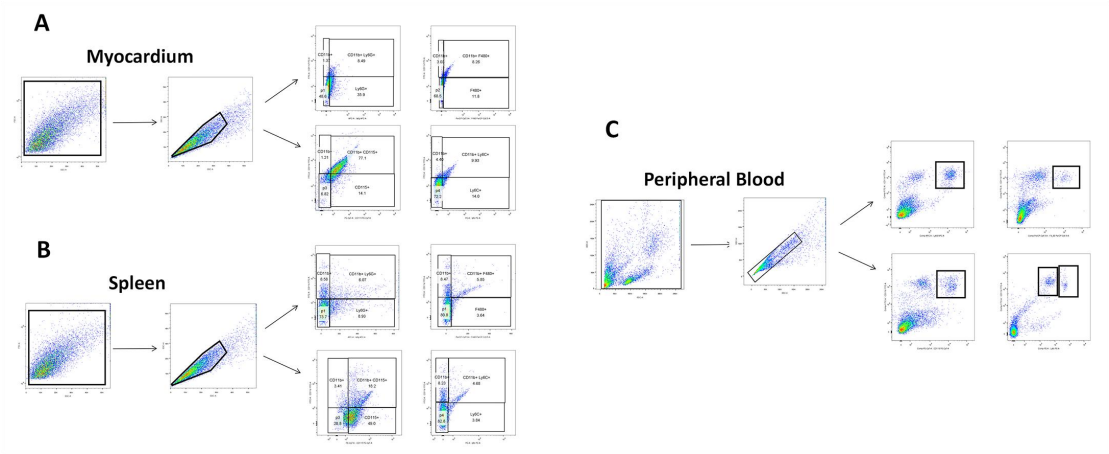

Figure S13. Gating strategies for cardiac, spleen, and peripheral blood in flow cytometry analysis.

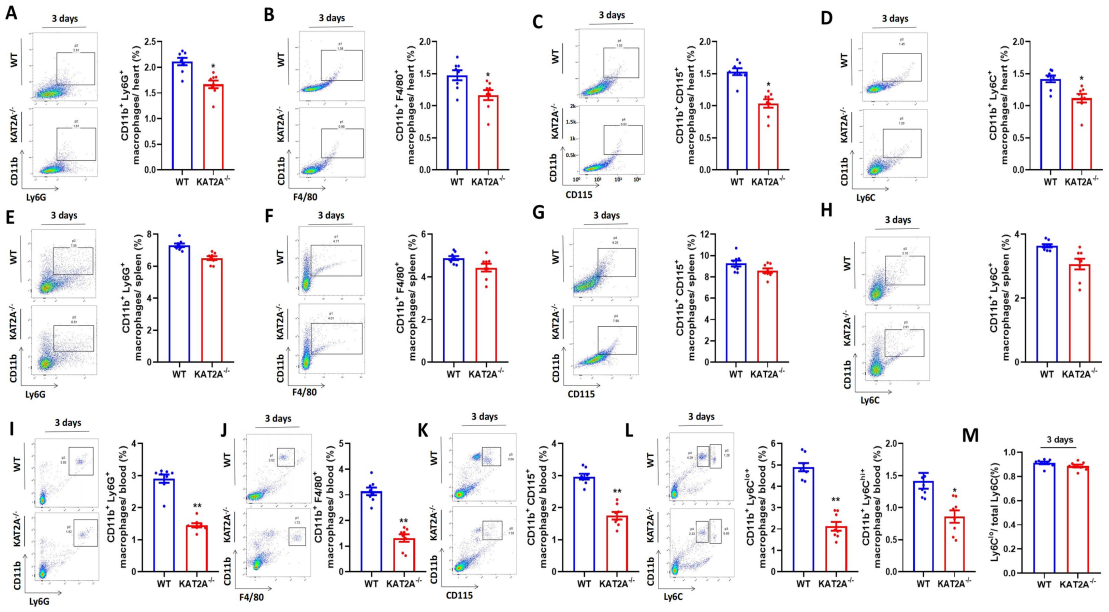

Figure S14. Effect of KAT2A deletion on immune cell recruitment 7 days after acute myocardial infarction (AMI) in spleen. AMI model was established using KAT2A$^{-/-}$ and wild-type (WT) mice to assess contents of CD11b^{+} Ly6G^{+} neutrophils (**A**), CD11b^{+} F4/80^{+} macrophages (**B**), CD11b^{+} CD115^{+} monocytes (**C**), and CD11b^{+} Ly6C^{+} monocytes (**D**). Data are expressed as means ± SEM, n = 8 in each group; $^{*}P <$ 0.05, $^{**}P <$ 0.01 versus WT group. Unpaired Student's t-test for comparing two groups.

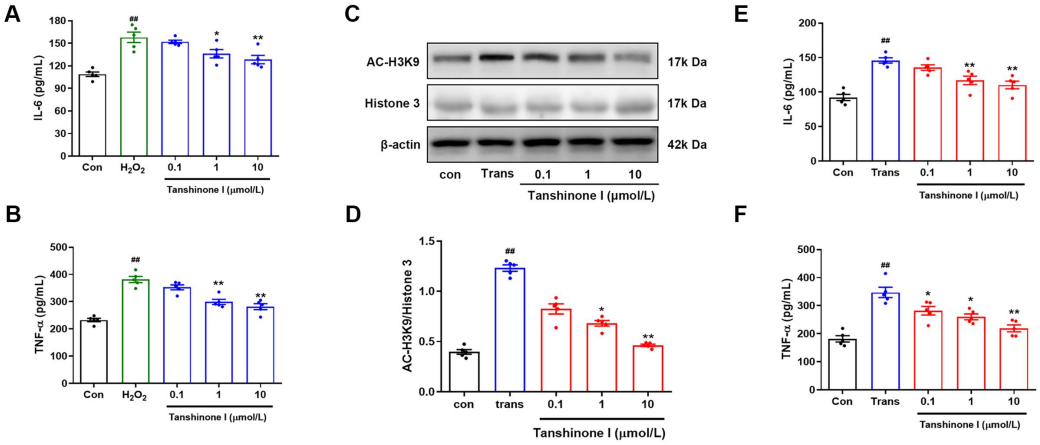

Figure S15. Tanshinone I significantly suppresses KAT2A function. (**A-B**): The effect of Tanshinone I on interleukin-6 (IL-6) (**A**) and tumor necrosis factor-α (TNF-α) (**B**) expressions after cellular injury induced by H_2O_2. (**C-D**): Changes in AC-H3K9 expression in cells after treatment with Tanshinone I. Tanshinone I (10 μmol/L) inhibited the increased KAT2A expression. (**E-F**): The effect of Tanshinone I on IL-6 (**E**) and TNF-α (**F**) expressions after KAT2A over expression. The data are expressed as mean ± SEM, n=5 in each group; $^{\#\#}P<0.01$ versus control; $^{*}P<0.05$, $^{**}P<0.01$ versus model. Unpaired Student's t-test for comparing two groups, and two-way ANOVA was used for comparing multiple groups.

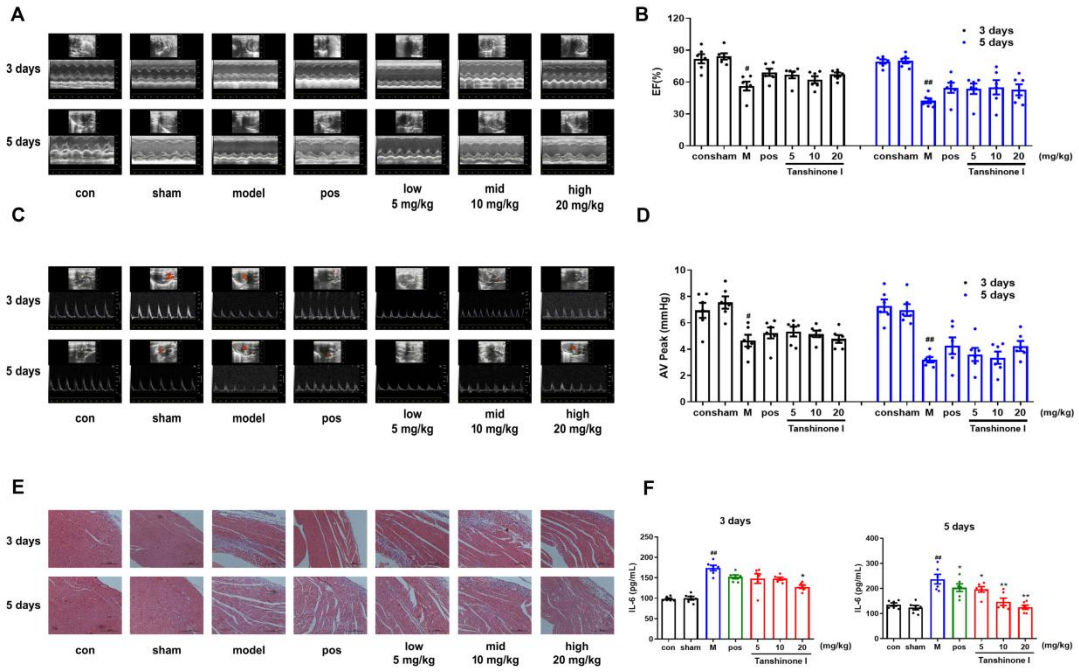

Figure S16. Tanshinone I can significantly ameliorate cardiac function and inhibit the inflammatory response following acute myocardial infarction (AMI). (**A**-**B**): Effects of Tanshinone I on cardiac function. Quantitative assessment of dilation and systolic function based on left ventricular ejection fraction. (**C**-**D**): Effects of Tanshinone I on the hemodynamic index. Quantitative assessment of hemodynamic index based on arteriovenous peak. Ejection fraction and arteriovenous peak were significantly larger in rats administered Tanshinone I (10 and 20 mg/kg) after 3 and 5 days, respectively, than in those treated with saline. (**E**): Representative photomicrographs of hematoxylin and eosin–stained myocardium (100×). Arrows indicate damaged areas. Tanshinone I significantly ameliorated cardiac function. (**F**): Interleukin-6 were markedly upregulated in the treated AMI model group (Tanshinone I 10 and 20 mg/kg) for 5 days and started being significantly downregulated thereafter. Data are expressed as mean ± SEM, n=6 in each group; $^{\#}P<0.05$, $^{\#\#}P<0.01$ versus sham; $^{*}P<0.05$, $^{**}P<0.01$ versus model. Unpaired Student's t-test for comparing two groups, and two-way ANOVA was used for comparing multiple groups.

Table S1. Characteristics of the included studies in the Meta-analysis

Author (pub. year)	Study setting	drugs	dosage	administratin protocol/Duration	Inflammatory biomarkers
Abbate et al. (2010)	USA	Anakinra	100 mg	subcutaneously once daily,14 days	white blood cell counts (↓), absolute neutrophil counts (↓), C-reactive protein (↓)
Abbate et al. (2015)	USA	Prolastin C	60 mg/kg	single infusion	C-reactive protein (↓)
Akbulut et al. (2009)	Turkey	Clopidogrel	75 mg	orally once daily,6 days	hs C-reactive protein (↓)
Chen et al. (2016)	China	Liraglutide	0.6 mg/1.2 mg/1.8 mg	2 days/2 days/3 days,each patient received seven injections	hs C-reactive protein (↓), interleukin-6 (↓)
Correia et al. (2003)	Brazil	Atorvastatin	80 mg	orally once daily,5 days	C-reactive protein (↓)
Doi et al. (2014)	Japan	Eicosapentaenoic acid	1800 mg/day	for 30 days	C-reactive protein (↓)
Ercan et al. (2004)	Turkey	Tirofiban	0.4 μg/kg /0.1 μg/kg	bolus per minute over 30 minutes/bolus per minute for 48 hours	hs C-reactive protein (↓)
Gao et al. (2018)	China	Ticagrelor/ Clopidogrel	loading dose (maintenance dose): 180 mg(90 mg)/ 600 mg (75 mg)	twice daily/ once daily	hs C-reactive protein (↓), interleukin-6 (↓)
Gavazzoni et al. (2017)	Italy	Atorvastatin	80 mg/20 mg	once daily, 1 mouth	hs C-reactive protein (↓), interleukin-6 (↓), TNF-α (↓)

Table S1. Characteristics of the included studies in the Meta-analysis (continue)

Author (pub. year)	Study setting	drugs	dosage	administratin protocol/Duration	Inflammatory biomarkers
Gong et al. (2018)	China	Captopril& Valsartan& Aspirin	18 mg& 80mg& 100 mg	once daily, 6 mouth	hs C-reactive protein (↓), interleukin-6 (↓), TNF-α (↓)
Gruzdeva et al. (2016)	Russia	Atorvastatin	20 mg	orally once daily,12 days	C-reactive protein (↓), interleukin-6 (↓)
Guazzi et al. (2007)	Italy	Atorvastatin	20 mg	orally once daily,12 weeks	C-reactive protein (↓)
Lekakis et al. (2006)	Greece	Rofecoxib	25 mg	orally once daily,7 days	C-reactive protein (↓), interleukin-6 (↓)
Morton et al. (2015)	UK	Anakinra	100 mg	subcutaneously once daily,14 days	C-reactive protein (↓), interleukin-6 (↓)
Ren et al. (2017)	China	Rosuvastatin& ezetimibe	10 mg&10 mg	orally once daily,1 year	hs C-reactive protein (↓), Lp-PLa2 (↓)
Sonnino et al. (2014)	USA	Anakinra	100 mg	subcutaneously once daily,14 days	interleukin-6 (↓)
Sposito et al. (2011)	Brazil	Simvastatin	20, 40, or 80 mg/day starting at admission; or 80 mg/day for 48 hours after admission. After 7 days, 20 mg/day for an additional 3 weeks		C-reactive protein (↓), interleukin-2 (↓), TNF-α (↓)

Table S2. Binding energy of nature compounds and KAT2A

Ingredients	Compounds	Binding energy with KAT2A (kcal/mol)
Astragaloside A	$C_{41}H_{68}O_{14}$	-9.13
Calycosin	$C_{16}H_{12}O_5$	-7.51
Ferulic acid	$C_{10}H_{10}O_4$	-5.31
Ononin	$C_{22}H_{22}O_9$	-2.52
Oleanolic acid	$C_{30}H_{48}O_3$	-8.79
Ursolic acid	$C_{30}H_{48}O_3$	-8.10
luteolin	$C_{15}H_{10}O_6$	-6.76
Wedelolactone	$C_{16}H_{10}O_7$	-6.12
Paeoniflorin	$C_{23}H_{28}O_{11}$	-2.18
Notoginsenoside R1	$C_{47}H_{80}O_{18}$	-4.15
HYA	$C_{27}H_{32}O_{16}$	-4.23
Tanshinone I	$C_{19}H_{18}O_3$	-8.45
Salvianolic acid C	$C_{26}H_{20}O_{10}$	-8.41
Tanshinone IIA	$C_{19}H_{18}O_3$	-7.98
Salvianolic acid A	$C_{26}H_{22}O_{10}$	-7.90
Danshensu	$C_9H_{10}O_5$	-5.32
Ligustrazine	$C_8H_{12}N_2$	-4.96
Ligustilide	$C_{12}H_{14}O_2$	-4.67
Protocatechuic acid	$C_7H_6O_4$	-4.63
Senkyunolide I	$C_{12}H_{16}O_4$	-3.13
Ginsenoside Rg3	$C_{42}H_{72}O_{13}$	-8.13
Ginsenoside Re	$C_{48}H_{82}O_{18}$	-7.18
Ginsenoside Rg1	$C_{42}H_{72}O_{14}$	-7.08
Quercetin	$C_{16}H_{18}O_9$	-5.33
Geniposide	$C_{17}H_{24}O_{10}$	-5.20
Eucommin A	$C_{15}H_{22}O_9$	-4.98
Glycyrrhizic acid	$C_{42}H_{62}O_{16}$	-3.19